Science Forum (Journal of Pure and Applied Sciences)

Journal Homepage: https://atbuscienceforum.com.ng/index.php/jpas

Formation evaluation and reservoir characterization of hydrocarbon sand units in "X Field" Onshore Niger Delta Basin

Edward Ozah[1], Dulu Appah[1], Richmond Ideozu[2] and Eze Okoro[3*]

[1] Center for Petroleum Geosciences, University of Port Harcourt, Nigeria.

[2] Department of Geology, University of Port Harcourt, Nigeria.

[3] Department of Geology, University of Nigeria Nsukka.

Abstract

This study investigates the hydrocarbon potential and reservoir quality of sand units within the "X" Field, located onshore in the Niger Delta Basin, through the integrated analysis of wireline log data and core samples. Composite log suites—including gamma ray, resistivity, neutron, density, and sonic logs—from three representative wells were interpreted to evaluate subsurface lithology, fluid types, and key petrophysical parameters relevant to hydrocarbon exploration and production. Two principal reservoir units encountered at varying depth intervals across the wells were identified and designated as the E_7000 and F_9000 Sands. Petrophysical evaluation revealed that these units comprise good-quality sandstone reservoirs, with average effective porosity (Øe) values ranging from 10% to 25%, and net-to-gross (N/G) ratios between 31% and 85%. Crossplot analyses of log-derived data aided in lithology discrimination, effectively separating sand-dominated and shale-dominated intervals, and indicating hydrocarbon saturation—primarily oil and gas—in the reservoir sands. Integration with core data allowed for a more robust lithofacies and depositional environment interpretation, suggesting a transition from shoreface to fluvio-deltaic and submarine depositional systems. Among the identified units, the Sand A interval within the E_7000 Sand exhibited the best reservoir properties, with an average effective porosity of 23% and a net-to-gross ratio of 80%, indicating excellent reservoir potential. The study further observed a general decline in reservoir quality with increasing depth, attributed to enhanced compaction, cementation, and heterogeneity within deeper stratigraphic intervals—common characteristics of deeper sections of the Niger Delta Basin. These findings underscore the importance of integrating core and wireline log data for accurate reservoir characterization, and they provide critical insights for optimizing field development and hydrocarbon recovery in the region.

Keywords
Formation evaluation,
Reservoir characterization,
Hydrocarbon sand units,
Niger Delta Basin

Corresponding Author: Edward Ozah, Center for Petroleum Geoscience, University of Port Harcourt. Nigeria, Email: eddyozah@gmail.com

INTRODUCTION

Most oil and gas reservoirs within the onshore Niger Delta Basin are already beyond their peak stages, and are current experiencing production decline due to long term exploitation. The need to extend the economic life of these mature fields requires detailed description of the reservoir characteristics to ascertain their hydrocarbon producibility, in order to shore-up Nigeria's depleting hydrocarbon reserves. The complex depositional setting of the Niger Delta Basin exerts huge control on reservoir properties distribution, introducing geological heterogeneities which makes accurate reservoir description difficult, and thus, poses high exploration risk. However, hydrocarbon recovery from brown fields can be improved by integrating wireline logs and core data to understand the continuity, extent, geometry, and distribution of the reservoir sand units (Han et al., 1986; Singh et al., 2013; Yu et al., 2016).

Formation evaluation is a vital technique employed to assess the producibility potential hydrocarbon-bearing reservoir units. The procedure includes wireline log interpretation to determine the formation petrophysical properties. Reservoir formation evaluation aims to determine key parameters like porosity, lithology, fluid saturations, permeability, and also make inferences on hydrocarbon presence. Essentially, wireline logs and core data are integrated identify the formations having greater promises to produce hydrocarbons in economic quantity (Mahmoud et al., 2023; Amer et al., 2025). Th present study utilizes wireline logs and core data for detailed formation evaluation of hydrocarbon-bearing sand units in the "X" Field onshore Niger Delta Basin to determine the production potentials of the reservoir intervals (Hassan et al., 2014; Chikiban et al., 2022; Amer et al., 2023; Eid et al., 2024; Lasheen et al., 2024). This will shed more light on the reservoir performance, reduce uncertainties in reserves estimations, and increase hydrocarbon productivity from the already explored heterogeneous sand sequences in the field (Ogbe et al., 2021; Opara et al., 2021, Okewu et al., 2024; Osaki, 2025).

2 Location and Geologic Setting

The studied field is located in the eastern part of Coastal Swamp Depobelt, Niger Delta Basin (Fig. 1). Evolution of the basin has been associated with the Early Cretaceous splitting of the Gondwana Supercontinent via a triple rift junction that connected the South Atlantic Ocean with the Benue depression which formed the failed arm of the tripartite rift system (Short and Stauble, 1967; Evamy et al., 1978; Uchupi, 1989; Doust and Omatsola, 1990). The Benue Trough experienced thermal cooling and sagging (drifting stage) during the late Eocene, paving way for the Niger Delta Basin to fully develop over the passive continental margin of West Africa through to the present day. With an arial coverage of about 140,000 km^2, the basin received approximately 12 km thick wedge of sediments supplied by the Niger and Benue Rivers (Reijers, 2011) and deposited onto the subaerial fluvio-deltaic environments and the related deepwater fans/channel systems (Cohen and McClay, 1996; Corredor et al., 2005; Briggs et al., 2006; Zhang et al., 2022). The diachronous lithostratigraphic successions of the Niger Delta Basin are divided into three, namely: the Akata Formation, Agbada Formation, and Benin Formation (Fig. 2). The lithological formations reflect a transition from prodeltaic (marine) shales through delta front - submarine clastics to continental sands in the onshore part of the basin (Corredor et al., 2005).

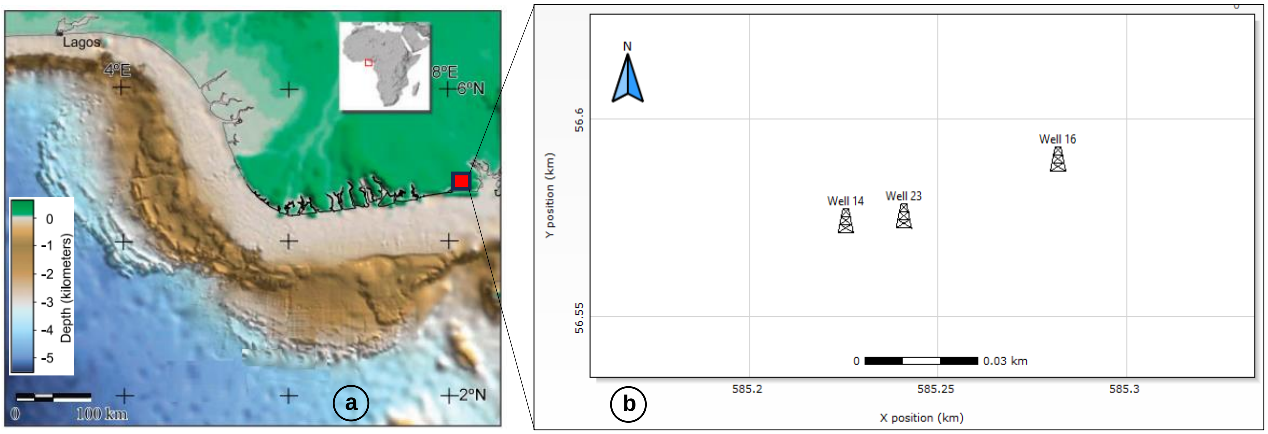

Fig. 1. (a) High-resolution bathymetric image of the Niger Delta showing the studied field in red box (after Corredor et al., 2005). (b) Base map of the field showing the three wells evaluated in this study.

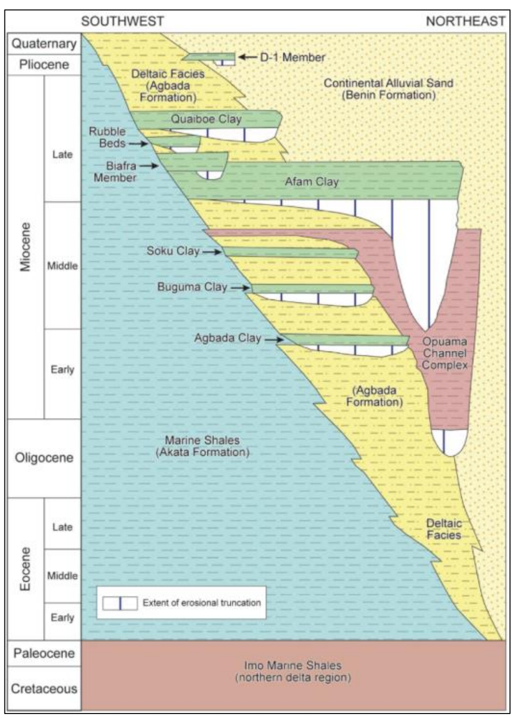

Fig. 2. Regional stratigraphy of the Niger Delta basin (after Doust and Omatsola, 1990; Chima et al., 2019).

3 Materials and Methods

3.1 Dataset

The dataset used for this study was made available by the Nigerian Upstream Petroleum Regulatory Commission (NUPRC). These include the following:

1. composite log suites from three (3) wells, comprising of gamma ray, resistivity, neutron, density, and sonic logs.
2. core (photos) data for one well (Well 14)
3. well header and deviation files

Summary of the log suites that were provided for this study are shown in Table 1. The well log suites were quality checked for data inconsistencies and corrections applied where necessary, before loading them into the appropriate software for analysis and interpretation. The log quality is generally good with all wells having gamma ray and resistivity, and at least one or more of the porosity logs (sonic, neutron, density).

3.2 Methods

Detailed evaluation of the available well log and core data involved the following processes: log lithofacies identification, depositional environment interpretation, well log correlation, and petrophysical properties estimation, following the workflow outlined in classical literature (e.g., Schlumberger, 1989; Rider, 2002; Asquith and Krygowski, 2004; Tiab and Donaldson, 2015). The inter-disciplinary approach adopted in this study is summarized in the interpretation workflow provided in figure 3.

Table 1. Summary of the available well and core data used for petrophysical analysis.

FIELD	WELLS		LOG SUITE					CORE
	HEADER	DEV	GR	RES	DEN	NEU	SON	
X	WELL 14	★ Yes	★ Yes	★ Yes	★ Yes	★ Yes	★ Yes	★ Yes
	WELL 16	★ Yes	★ Yes	★ Yes	★ Yes	★ Yes	★ Yes	★ No
	WELL 23	★ Yes	★ Yes	★ Yes	★ Yes	★ Yes	★ Yes	★ No

★ Yes
★ No

3.2.1 Lithofacies and Depositional Environment Analysis

The identification of lithofacies and depositional environments of the sediments encountered in the evaluated wells was done by analyzing the signature of the gamma ray logs to establish the interactions between various environments that left their imprints on the sedimentary deposits. Lithofacies display a distinct character and appearance that replicates the predominant conditions that formed them, and which distinguishes them from adjacent or associated rock units. Thus, the observed characteristics of a lithofacies gives clue to the depositional conditions and environments in which the sediments were formed (Selley, 1985; Murkute, 2001). In this study, the signatures of gamma ray logs were employed to make inferences on the grainsize variations of the sediments and depositional energy. The lithofacies analysis was constrained by the available core photos to establish the prevailing depositional environments in the study area. The depositional environments interpretation model adopted in this study followed the proposition of Emery and Myers (1996).

3.2.2 Well Correlation

Correlation of the wells was achieved by identifying and mapping prominent shale markers that showed distinct high gamma ray log signatures. This enabled appropriate and easy delineation of reservoir sand units of interest. For this purpose, the gamma ray and resistivity logs were integrated, while the neutron and density logs were used identify hydrocarbon-bearing sand units in the field.

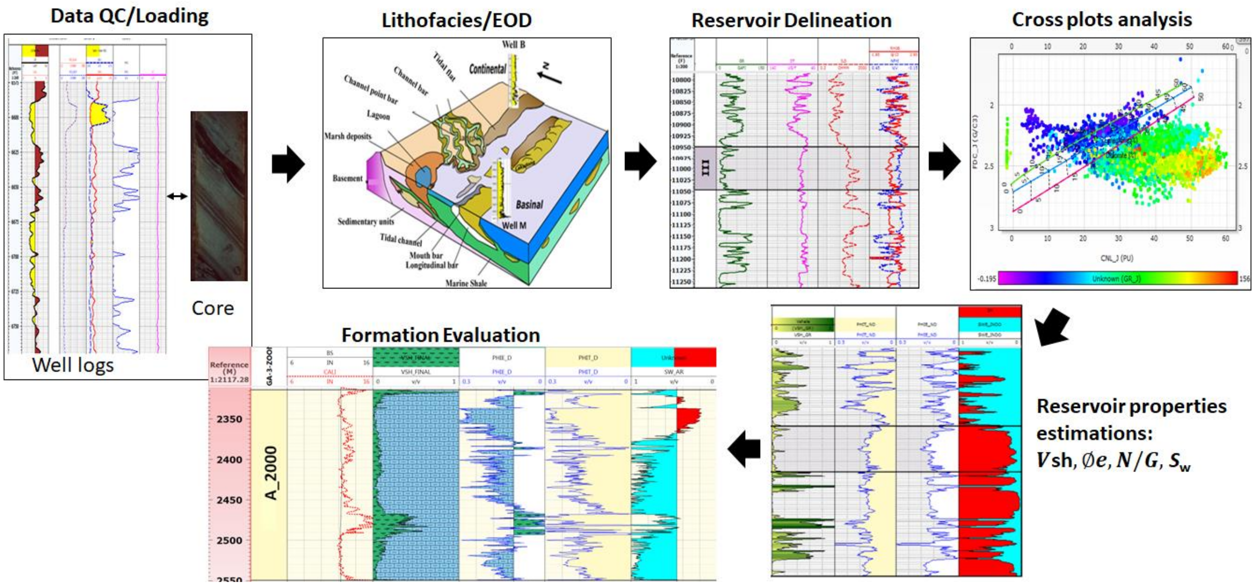

Fig. 3. Summary of the well logs and core data interpretation workflow.

3.2.3 Calculation of Petrophysical Parameters

Computation of petrophysical properties like volume of shale (V_{sh}), net-to-gross ratio (NTG), water saturation (S_w) and effective porosity ($\emptyset_e$) for the delineated reservoir intervals was achieved using standard empirical equations. This was done to capture the lateral and vertical distribution of reservoir parameters across the field. The equations used in calculating the petrophysical properties are as follows 9 (Asquith and Krygowski, 2004):

$$\emptyset_{den} = \frac{(\rho_m - \rho_b)}{(\rho_m - \rho_b)} \qquad (1)$$

where ρ_b is the bulk density derived from log measurement, ρ_f is the fluid density, ρ_m is the matrix density, and $\emptyset_{den}$ is the porosity value derived from the density log. We used equation 1 to compute the total porosity for the identified reservoirs of interest.

The volume of shale (V_{sh}) was estimated using the Larionov (1969) algorithm which accounts for the proportion of shale in a heterolithic reservoir or a sandstone:

$$V_{sh} = 0.083 * (2^{3.7*I_{GR}} - 1) \qquad (2)$$

where the gamma ray index (I_{GR}) is given by:

$$I_{GR} = \frac{(GR_{log} - GR_{min})}{(GR_{max} - GR_{min})} \quad (3)$$

GR_{log} is the gamma ray log value, GR_{min} is the lowest gamma ray log value derive from a sand interval, and GR_{max} is the highest gamma ray log value determined from a shale interval.

Water saturation in the reservoirs was calculated using the Simandoux (1963) model which performs better for typical shaly sand reservoirs like those of the Niger Delta Basin. It is given by:

$$\frac{1}{R_t} = \frac{\emptyset_e^m * S_w^n}{a * R_w} + \frac{V_{sh} * S_w}{R_{sh}} \quad (5)$$

where R_t is the true formation resistivity, $Ø_e$ is the effective porosity, S_w is the water saturation of the uninvaded zone, V_{sh} is the volume of shale, R_w is the resistivity of formation water, R_{sh} is the resistivity of shale, n is the saturation exponent, m is the cementation factor; and a is the tortuosity factor.

The net-to-gross (N/G) was estimated using Equation 6 to ascertain the ratio of the clean porous reservoir sand thickness (Net) to the overall (Gross) reservoir thickness:

$$N/G = IF(V_{sh} \leq 0.40, (1 - V_{sh}), 0) \quad (6)$$

The N/G values are not the same for a given a reservoir, and thus can vary between 1.0 for clean sand intervals to 0.0 for non-reservoir zones over a small distance.

Finally, the effective porosity (Øe) was calculated using the following equation:

$$\emptyset_e = (1 - V_{sh}) * Por_{den} \quad (7)$$

4 Results and Discussion

4.1 Facies and Depositional Environments Interpretation

The four lithofacies units identified in the study area is presented in figure 4. These include the Sandstones Facies, Shaly Sandstone Facies, Mudrock Facies, and Heterolithic Facies. Each of the facies depicted the prevailing processes and conditions under which they were formed, and exemplified marked characteristics that differentiates each of them from other related adjacent rock types. The observed gamma ray log signatures displayed by the lithofacies including bell, funnel, cylindrical, symmetrical, and serrated motifs gave clue on the vertical variations of grainsize profile in the sand and shale sequences.

The lithofacies, constrained with the available core photos, were used to make inferences on the environments of deposition in which the sediments were laid down (Fig. 5). For instance, the serrated motif suggests intercalation of shales and sandstone layers deposited by fluvial, tidal or marine processes. The bell-shaped signature suggests fining upward profile or an increase in shale content up section or an upward decrease in the depositional energy, characterized by fluvial channel systems. The funnel shaped pattern on the other hand replicates a coarsening upward profile or an upward decrease in shale content related to progradational deltaic sediments. The blocky of cylindrical motif suggests a coarse-grained sandstone of uniform thickness deposited by braided channel systems, tidal channel or subaqueous slump deposits.

4.2 Correlation of the Logs

Lithological correlation of the logs revealed two reservoir intervals designated as E_7000 Sand and F_9000 Sand (Fig. 6). The correlation of the three wells evaluated in this study aided in the isolation of non-reservoir shale units from the porous and permeable sand reservoir zones, and also enabled appropriate identification of the sand reservoirs saturated with hydrocarbon fluids. The sand reservoirs of interest were characterized by low gamma ray values and high resistivity kicks, suggesting the possibility of oil and gas saturation in them. The reservoir intervals also showed marked decrease in the density log reading and subsequent increase in the neutron log reading, culminating into the "ballon effect" due to the density-neutron log crossover. The mapped sand units containing hydrocarbons were further evaluated to ascertain their potentials to produce oil and gas in appreciable economic quantity.

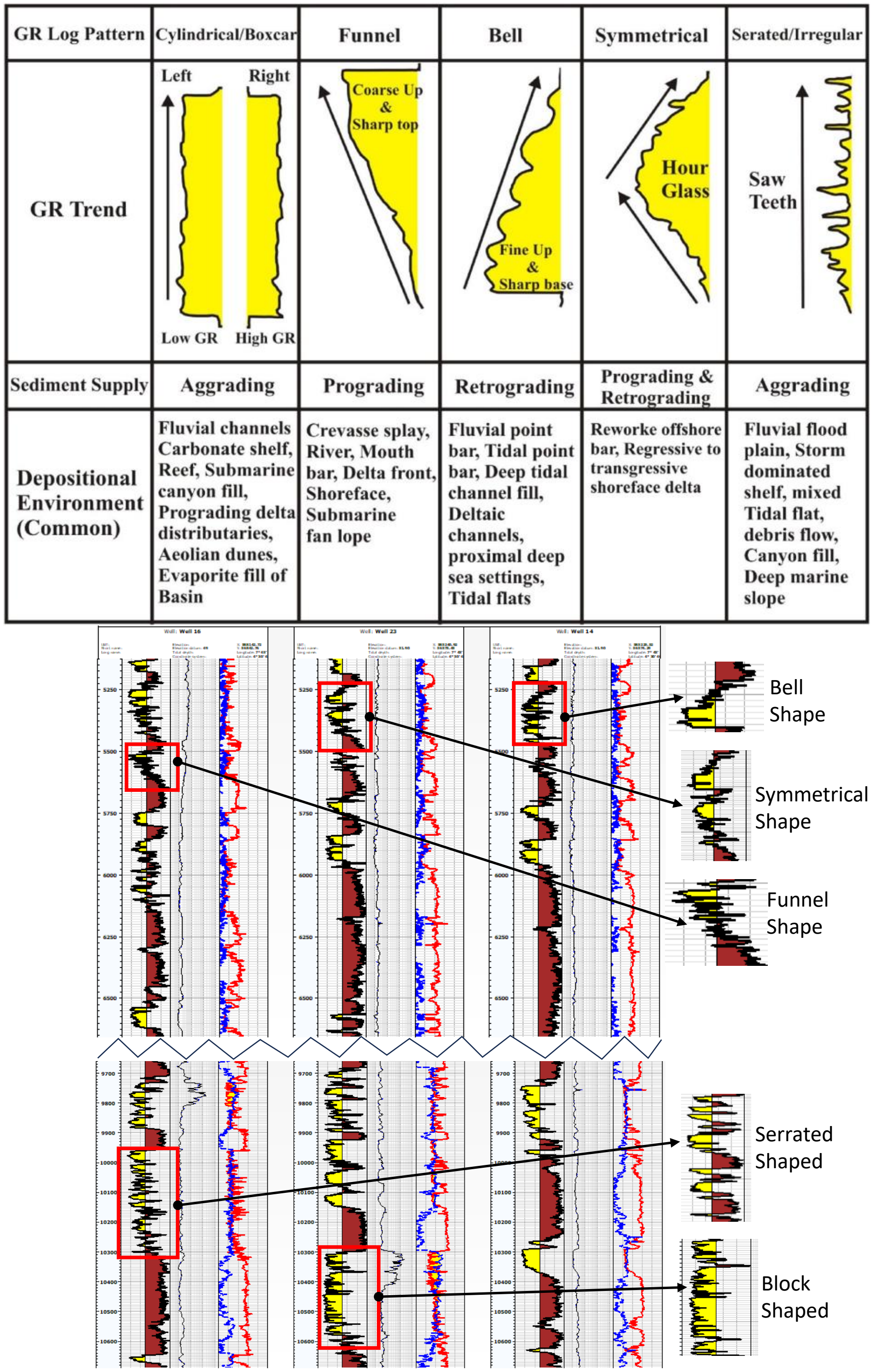

GR Log Pattern	Cylindrical/Boxcar	Funnel	Bell	Symmetrical	Serated/Irregular
GR Trend	Left, Right, Low GR, High GR	Coarse Up & Sharp top	Fine Up & Sharp base	Hour Glass	Saw Teeth
Sediment Supply	Aggrading	Prograding	Retrograding	Prograding & Retrograding	Aggrading
Depositional Environment (Common)	Fluvial channels Carbonate shelf, Reef, Submarine canyon fill, Prograding delta distributaries, Aeolian dunes, Evaporite fill of Basin	Crevasse splay, River, Mouth bar, Delta front, Shoreface, Submarine fan lope	Fluvial point bar, Tidal point bar, Deep tidal channel fill, Deltaic channels, proximal deep sea settings, Tidal flats	Reworke offshore bar, Regressive to transgressive shoreface delta	Fluvial flood plain, Storm dominated shelf, mixed Tidal flat, debris flow, Canyon fill, Deep marine slope

Fig. 4. Common sedimentological facies associated with various gamma ray logs (after Cant, 1992; Emery and Myers, 1996).

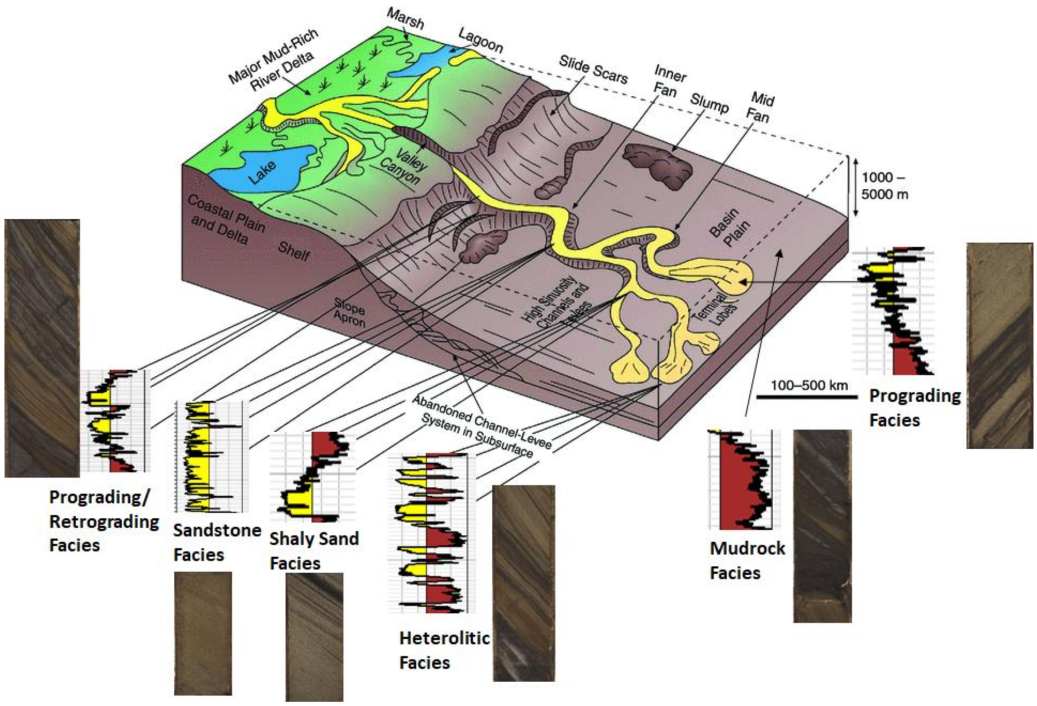

Fig. 5. Conceptual model showing that depositional facies and environments (after Shields et al., 2017)

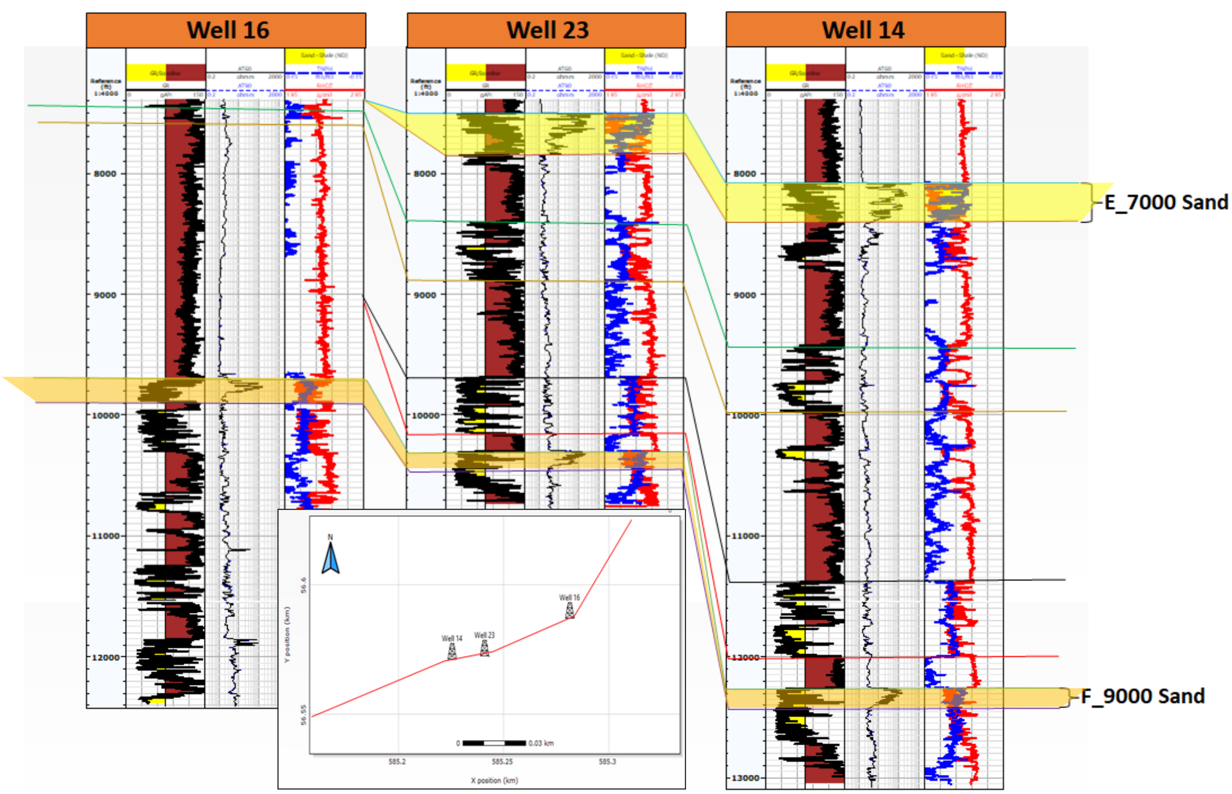

Fig. 6. Log correlation panel showing the delineated sand reservoir units.

4.3 Petrophysical Characterization of the Reservoir Zones

Tables 1 summarizes the estimated reservoir parameters for the two sand intervals of interest delineated in this study. The E_7000 Sand was encountered within the depth range of 8084.50 to 8340.22 ft in Well 14. This sand unit was also penetrated by Well 23 at the depth range of 7506.60 to 7670.04 ft. However, the E_7000 Sand appeared to be "shale out" up dip, and was not encountered in Well 16. On the other hand, the F_9000 Sand was penetrated by the three wells evaluated in this study. The reservoir occurred within the depth range of 12265.30 to 12363.70 ft in Well 14, and was encountered in Well 16 at depth ranging from 9732.66 to 9816.94 ft. In Well 23, The F_9000 Sand was penetrated at depths ranging 10300.10 to 10430.60 ft. A comprehensive description of the characteristics of the reservoirs are provided in the next headings.

Table 2. Summary of the estimated reservoir properties.

Name	Reservoir	Zone	Top (ft)	Base (ft)	Gross (ft)	Net (ft)	Av. N/G (v/v)	Av. Vsh (v/v)	Av. $Ø_e$ (v/v)	Av. Sw (v/v)
Well 14	E_7000	Sand A	8084.50	8114.10	29.60	26.80	0.75	0.20	0.25	0.21
		Sand B	8129.99	8232.91	102.92	66.96	0.56	0.45	0.18	0.21
		Sand C	8255.60	8340.22	84.62	26.95	0.31	0.69	0.10	0.58
	F_9000	-	12265.30	12363.70	108.40	93.6	0.79	0.21	0.12	0.22
Well 16	E_7000	Sand A	-	-	-	-	-	-	-	-
		Sand B	-	-	-	-	-	-	-	-
		Sand C	-	-	-	-	-	-	-	-
	F_9000	-	9732.66	9816.94	84.48	66.96	0.68	0.32	0.12	0.34
Well 23	E_7000	Sand A	7506.60	7544.00	37.40	35.32	0.85	0.15	0.20	0.15
		Sand B	7555.00	7610.00	37.40	35.32	0.60	0.40	0.16	0.15
		Sand C	7635.83	7670.04	34.21	21.52	0.38	0.62	0.12	0.50
	F_9000	-	10300.10	10430.60	130.50	120.40	0.81	0.19	0.11	0.30

4.3.1 E_7000 Sand

The E_7000 Sand was penetrated by Well 14 and Well 23. The reservoir is sub-divided into three zones designated as Sand A, Sand B, and Sand C (Fig. 7). Sand A zone occurred in Well 14 at depths ranging from 8084.50 to 8114.10 ft, with gross thickness of 29.60 ft and net thickness of 26.80 ft. In Well 23, the Sand A zone was encountered at the depth of 7506.60 to 7544.00 ft, with gross thickness of 37.40 ft and net thickness of 35.32 ft. The estimated average net-to-gross ratio of over 70 %, average effective porosity of more than 20 %, and the average low water saturation values (less than 25 %) suggests that this reservoir zone is a high-quality sand unit with significant hydrocarbon saturation (up to 70 %). The density - neutron crossplot of this sand interval showed the possible fluid saturation to be gas. This is supported by the "gas effect" due to density – neutron crossover associated with the sand zone (Fig. 8).

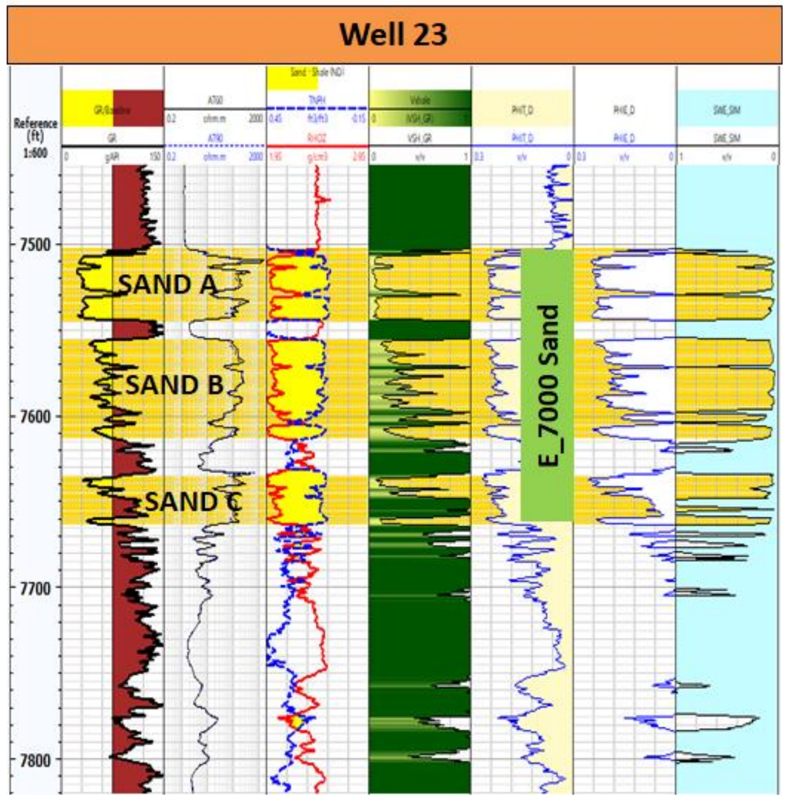

Fig. 7. Lithology plot of Well 23 showing the three reservoir zones of E_7000 Sand interval.

The Sand B zone was encountered in Well 14 at the depth range of 8129.99 to 8232.91 ft, with gross thickness of 102.92 ft and net thickness of 66.96 ft. It occurred at depths ranging from 7555.00 to 7544.00 in Well 23, with gross thickness of 37.40 ft and net thickness of 35.32 ft. This reservoir zone is characterized by average effective porosity greater than 16 % and average net-to-gross ratio of over 50 %. The average low saturation content (less than 20 %) is an indication that this sand unit is saturated with a significant volume of hydrocarbon, possibly gas, due to the marked density-neutron crossover observed at this interval. The density-neutron crossplot of this reservoir interval revealed the presence of gas, resulting in the over-shooting of the cluster point beyond the sandstone line (Fig. 9).

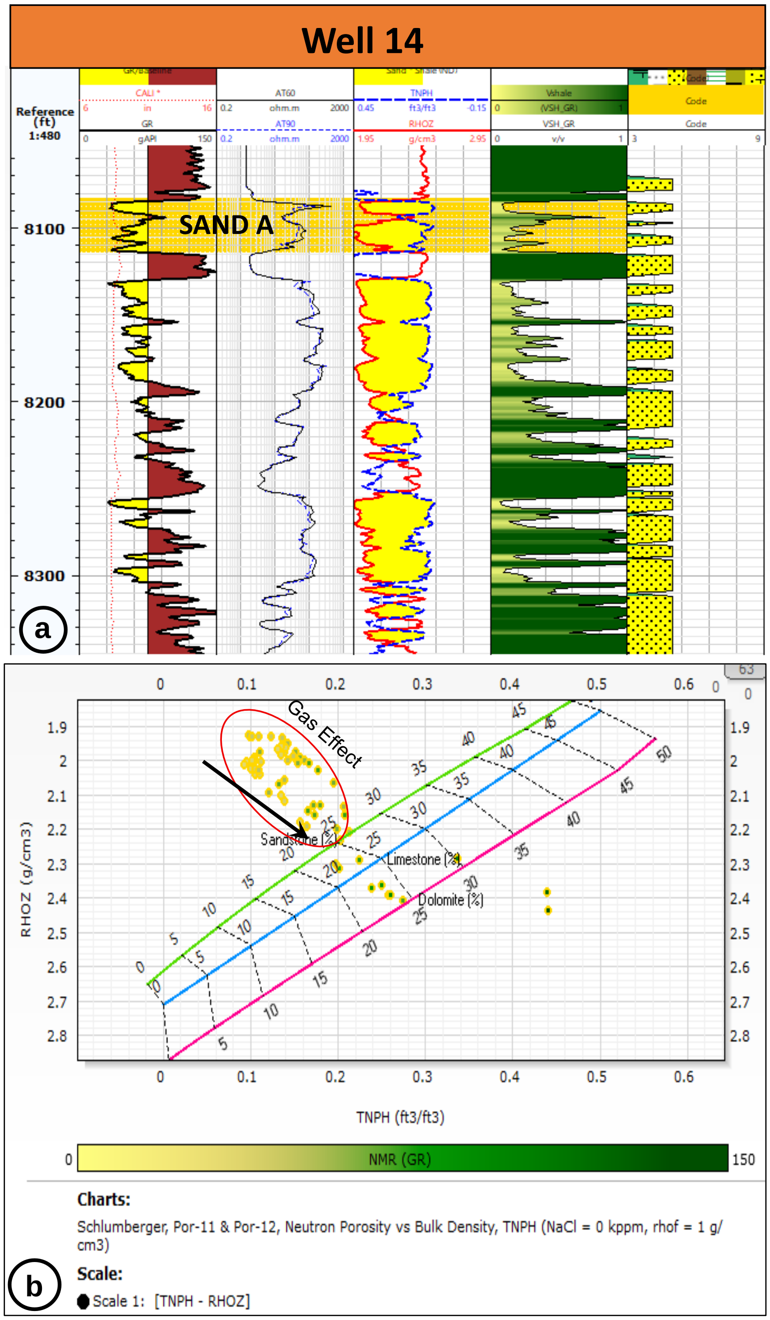

Fig. 8. (a) Lithology plot of Well 14 showing the Sand A zone. (b) Density-neutron crossplot of the Sand A zone.

Sand C zone was penetrated by Well 14 at the depth range of 8255.60 to 8340.22 ft, with gross thickness of 84.62 ft and net thickness of 26.95 ft. It occurred in Well 23 at the depth range of 7635.83 to 7670.04 ft, with gross thickness of 34.21 ft and net thickness of 21.52 ft. The sand unit is characterized by average net-to-gross ratio of lower than 40 %, average effective porosity of about 11 %, suggesting that it has fair to good reservoir quality. The estimated water saturation value of about 50 % indicates that the it is saturated with hydrocarbon fluid. The crossplot of density and neutron logs indicated possible gas saturation for the Sand C zone (Fig. 10). Core data retrieved from this sand interval between the depth of 8295 to 8320 ft showed a general coarsening upward grainsize variations for the reservoir which comprises mainly of sand-shale intercalations, typical of Heterolithic Facies (Fig. 11). This suggests that the sediments were deposited in a tidal-influenced outer delta front and shallow marine environments (Doust and Omatsola, 1990; Reijers, 2011).

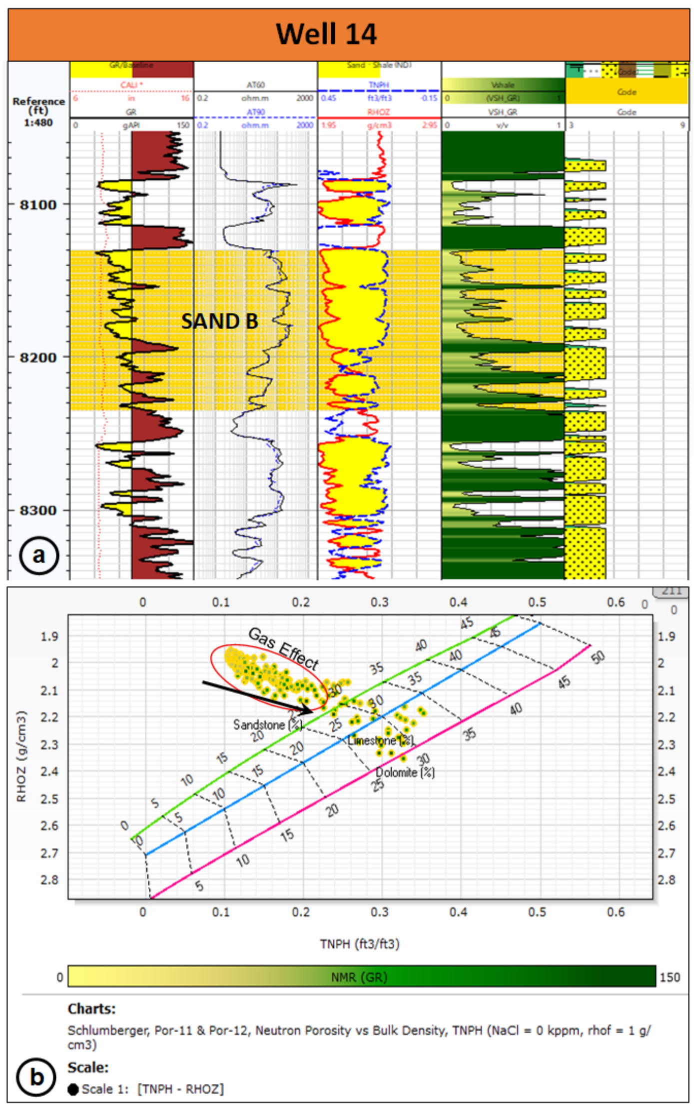

Fig. 9. (a) Lithology plot of Well 14 showing the Sand B zone. (b) Density-neutron crossplot of the Sand B zone.

4.3.2 F_9000 Sand

The F_9000 Sand was penetrated by all the three wells evaluated in this study (Fig. 6). In Well 14, the reservoir occurred at the depth range of 12265.30 to 12363.70 ft, with gross thickness of 108.40 ft and net thickness of 93.60 ft. It was intersected in Well 16 at the depth range of 9732.66 to 9816.94 ft, with gross thickness of 84.48 ft and net

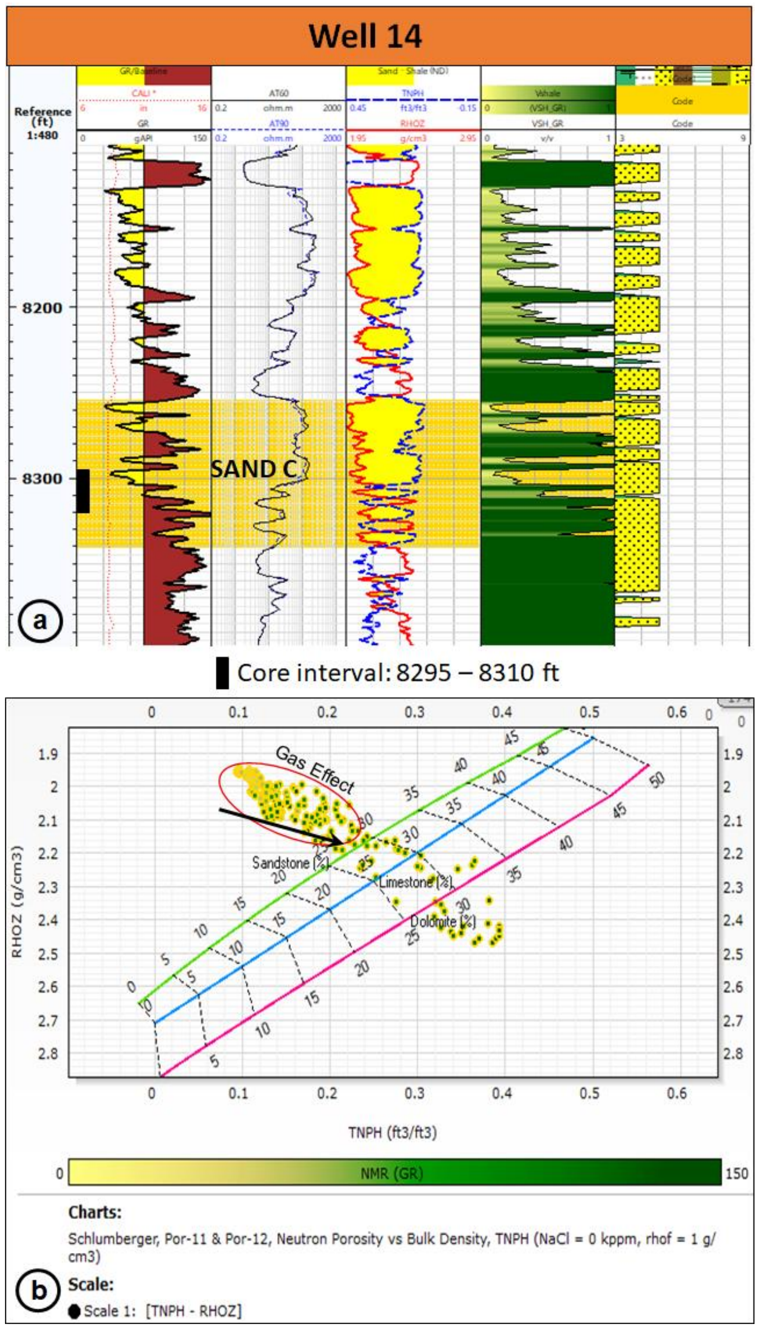

Fig. 10. (a) Lithology plot of Well 14 showing the Sand C zone with core data calibration. (b) Density-neutron cross plot of the Sand C zone.

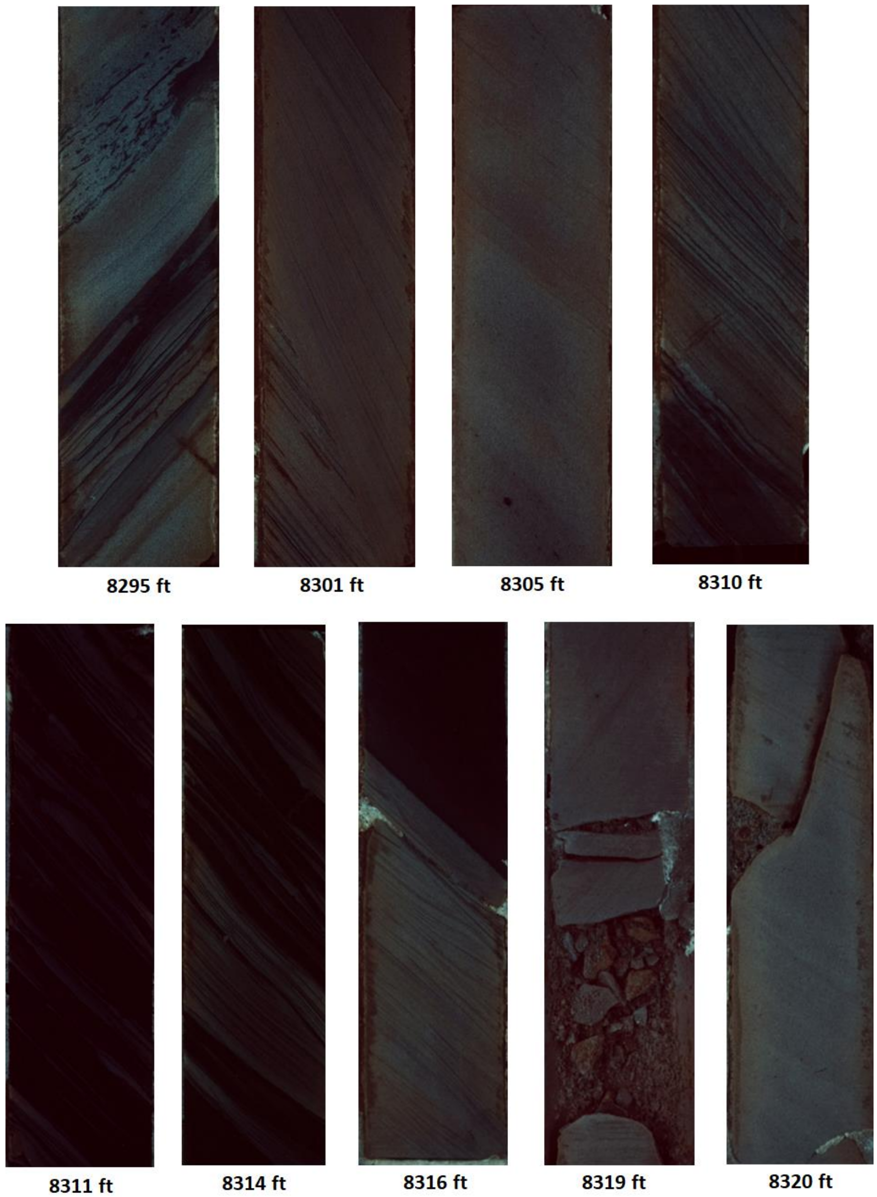

Fig. 11. Core photos of the Sand C interval (8295 to 8320 ft) show the lithofacies type in Well 14.

thickness of 66.96 ft. The reservoir was encountered in Well 23 at depth ranging from 10300.10 to 10430.60 ft, with gross thickness of 130.50 ft and net thickness of 120.40 ft. The estimated average net-to-gross ratio of more than 60 % and average effective porosity of approximately 12 % classifies the reservoir quality to be good. The low average water saturation value (less than 30 %) suggests that it is saturated by over 60 % hydrocarbon. The density – neutron crossplot for this sand interval indicates the possible fluid saturation to be oil (Fig. 12).

Based on the estimated petrophysical properties of the hydrocarbon-bearing reservoir intervals, the Sand A zone of

E_7000 Sand has the best reservoir quality with an overall net-to-gross ratio value of 80 %, effective porosity value of 23 %, and water saturation value of 28 % (Table 3).

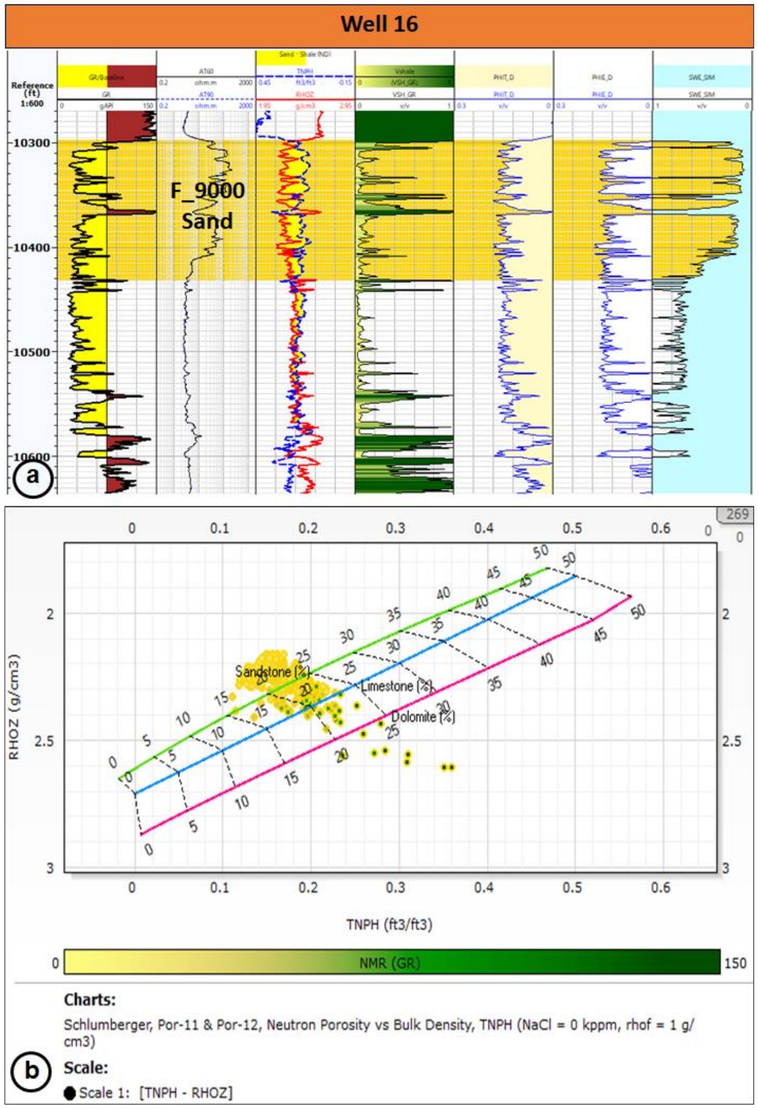

Fig. 12. (a) Lithology plot of Well 16 showing the F_9000 Sand. (b) Density-neutron crossplot of the F_9000 Sand.

Table 3. Summary of Overall Average Reservoir Quality Parameters.

	Reservoir	Zone	N/G (v/v)	Øe (v/v)	Sw (v/v)
Overall Average	**E_7000 Sand**	Sand A	0.80	0.23	0.18
		Sand B	0.58	0.17	0.18
		Sand C	0.35	0.11	0.54
	F_9000 Sand	-	0.76	0.12	0.29

5 Conclusion

Formation evaluation and characterization of reservoir sand units in the X Field, onshore Niger Delta Basin have been attempted in this study, with the view to ascertain their hydrocarbon potential of the identified sand zones. Based on the integrated interpretation of wireline logs and core data, four lithofacies units representing the interaction between different sub environments ranging from shoreface, through fluvio-deltaic to submarine depositional systems, were delineated. Lithological correlation of the logs revealed two reservoir intervals, designated as E_7000 Sand and F_9000 Sands, at different depths in the three wells evaluated in this study. Lithology crossplots of density and neutron logs showed that the reservoirs consist of sandstones, with varying shale intercalations. The computed petrophysical properties showed that the Sand A zone of the E_7000 Sand has the best quality, with an overall average net-to-gross ratio value of 80 % and effective porosity of 23 %. The low water saturation (18 %) in the sand unit is an indication that it is hydrocarbon saturated. In general, the overall quality of the reservoirs decreases with depth due to the increasing geological complexities and heterogeneities at greater depths in the Niger Delta Basin.

References

Amer, M., Mabrouk, W.M., Soliman, K.S., Noureldin, A.M. and Metwally, A., 2023. Three-dimensional integrated geo-static modeling for prospect identification and reserve estimation in the middle Miocene multi-reservoirs: a case study from Amal Field, Southern Gulf of Suez Province. Nat. Resour. Res., 32, pp. 2609 - 2635.

Amer, M., Mabrouk, W.M., Eid, A.M. and Metwally, A., 2025. Petrophysical assessment of the Hammam Faraun, Matulla and Nubia Reservoirs in the Ashrafi Oil Field, Gulf of Suez. Scientific Reports, 15:3326, pp. 1 – 21.

Asquith, G. and Krygowski, D., 2004. Basic Well Log Analysis. AAPG Methods in Exploration Series, 16.
Manchester, United Kingdom. 2, 23-59.

Briggs, S.E., Davies, R.J., Cartwright, J.A. and Morgan, R., 2006. Multiple detachment levels and their control on fold styles in the compressional domain of the deep-water west Niger Delta. Basin Research, 18, 435 - 450.

Cant, D., 1992. Subsurface facies analysis. In: Walker RG (ed) Facies models, response to sea level changes. Geological Association of Canada, St. Johns, 27 – 45.

Chikiban, B., Kamel, M.H., Mabrouk, W.M. and Metwally, A., 2022. Petrophysical characterization and formation evaluation of sandstone reservoir: case study from Shahd field, Western Desert, Egypt. Contrib. Geophys. Geodesy., 52, 443 - 466.

Chima, K.I., Do Couto, D., Leroux, E., Gardin, S., Hoggmascall, N., Rabineau, M., Granjeon, D. and Gorini, C., 2019. Seismic stratigraphy and depositional architecture of Neogene intraslope basins, offshore western Niger Delta. Marine and Petroleum Geology, 109, 449 - 468.

Cohen, H.A. and McClay, K., 1996. Sedimentation and shale tectonics of the northwestern Niger Delta front. Marine and Petroleum Geology, 13, 313 - 328.

Corredor, F., Shaw, J.H. and Bilotti, F., 2005. Structural styles in the deep-water fold and thrust belts of the Niger Delta. AAPG Bulletin, 89, 753 – 780.

Doust, H. and Omatsola, E., 1990. Niger delta. In: Edwards, J.D., Santogrossi, P.A. (Eds.), Divergent Passive Margin Basins, 48. AAPG Bulletin, pp. 239 - 248.

Eid, A.M., Mabrouk, W.M. and Metwally, A., 2024. Formation evaluation and petrophysical analysis of well logging data: an example from Matruh-Shushan Basin, North Western Desert, Egypt. Iraqi J. Sci., 2024, pp. 4336 - 4358.

Emery, D. and Myers, K., 1996. Sequence Stratigraphy. Blackwell, London, pp. 297.

Evamy, B.D., Haremboure, J., Kammerling, R., Knaap, W.A., Molloy, F.A. and Rowlands, P.H., 1978. Hydrocarbon habitat of Tertiary Niger Delta. AAPG Bull. 62, 1 - 39.

Han, D., Nur, A. and Morgan, D., 1986. Effects of porosity and clay content on wave velocities in sandstones. Geophysics, Vol. 51, pp. 2093 - 107.

Hassan, A.M., Mabrouk, W.M. and Farhoud, K.M., 2014. Petrophysical analysis for Ammonite-1 well, Farafra Area, Western Desert, Egypt. Arab. J. Geosci., **7**, 5107 - 5125.

Larionov, V. V. (1969). Borehole Radiometry, National Electric Drag Racing Association, Moscow, Soviet Union.

Lasheen, I., Noureldin, A.M. and Metwally, A., 2024. Reservoir characterization of the Abu Roash D Member through Petrography and seismic interpretations in Southern Abu Gharadig Basin, Northern Western Desert, Egypt. Sci. Rep., 14, 8966.

Mahmoud, A.I., Metwally, A.M., Mabrouk, W.M. and Leila, M., 2023. Controls on hydrocarbon accumulation in the pre-rift paleozoic and late syn-rift cretaceous sandstones in PTAH oil field, north Western Desert, Egypt: insights from seismic stratigraphy, petrophysical rock-typing and organic geochemistry. Mar. Pet. Geol., 155, 106398.

Murkute, Y.A., 2001. Kamthi sandstones: Grain size distribution and depositional processes. J. Geological Sos. India, 58, pp. 435 - 440.

Ogbe, O.B., Okoro, A.U., Ogagarue, D.O., Osokpor, J., Overare, B., Ocheli, A., Opatola, A.O. and Oluwajana, O.A., 2021. Reservoir hydrocarbon prospectivity and productivity evaluations of sands S-600 and S-700 of Fega field, onshore Niger Delta Basin, Nigeria. Journal of African Earth Sciences, 184: 1 – 12.

Okewu, G.O., Ugbor, D.O., Johnson, I., John, A.Y., Okoro, E.M. and Kentsa, T.S., 2024. Seismic Attributes Analysis and Petrophysical Evaluation of Reservoir Sand Units in "Mars" Field, Onshore Niger Delta Basin, Nigeria. Pet. Coal, 66(4): 1320 - 1336.

Opara, A.I., Okoro, E.M., Onyekuru, S.O., Njoku, I.O., Onyenegecha, C.P., Asedegbega, J.E., Ekwe, A.C., Okoli, A.E. and Ezekiel, J.C., 2021. Rock physics enhanced strati-structural interpretation of the "Wuzuzo Field", onshore Niger Delta, Nigeria, Upstr. Oil Gas Tech., 6, pp. 1 – 13.

Osaki, L.J., 2025. Assessing the Reservoir Quality and Prospectivity of the "MUH" Field, Onshore Niger Delta Basin. Pet. Coal, 67(2): 496 – 507.

Reijers, T.J.A., 2011. Stratigraphy and sedimentology of the Niger Delta. Geologos, 17(13), 133 - 162.

Rider, M., 2002. The Geological Interpretation of Well Logs. Blackie, Glasgow, 151 -165.

Selley, R.C., 1985. Elements of petroleum geology. W.H. Freeman and company, New York, pp. 448.

Schlumberger, 1989. Log Interpretation: Principles and Applications. Schlumberger Education Services Houston, 1-175.

Short, K.C. and Stauble, A.J., 1967. Outline of geology of Niger Delta. AAPG Bull. 51, 761 - 779.

Singh, V., Yemez, I. and Sotomayor, J., 2013. Key factors affecting 3D reservoir interpretation and modelling outcomes: industry perspectives. Br. J. Appl. Sci. Technol., Vol. 3, pp. 376 – 405.

Tiab, D. and Donalson, E.C., 2015. Petrophysics Theory and Practice of Measuring Reservoir Rock and Fluid Transport Properties. Gulf Professional Publishing, Elsevier, 1 – 898.

Uchupi, E., 1989. The tectonic style of the Atlantic Mesozoic rift system. Journal of African Earth Sciences, 8, 143 - 164.

Yu, C., Ji, S. and Li. Q., 2016. Effects of porosity on seismic velocities, elastic moduli and Poisson's ratios of solid materials and rocks. J. Rock Mech. Geotech. Eng., Vol. 8, pp. 35 – 49.

Zhang, J.-J., Wu, S.-H., Hu, G.-Y., Yue, D.-L., Chen, C., Chen, M., Yu, J.-T., Xiong, Q.-C. and Wang, L.-Q., 2022. Sedimentary - tectonic interaction on the growth sequence architecture within the intraslope basins of deep-water Niger Delta Basin. Journal of Palaeogeography, https://doi.org/10.1016/j.jop.2022.11.001.